Supplemental Information (ESI) for Chemical Communications

Electrochemically erasable hydrogen-bonded thin films

Daniel J. Schmidt[1] and Paula T. Hammond[1,*]

[1]*Department of Chemical Engineering, Massachusetts Institute of Technology, Cambridge, MA 02139, USA.*

*Corresponding author. E-mail: hammond@mit.edu. Fax: 617 258 5766; Tel: 617 258 7577

S1. Materials and Methods

S1.1 Materials

Polyvinylpyrrolidone (PVPON) (MW = 1.3 million), tannic acid (TA), polyallylamine hydrochloride (PAH) (MW = 70K), poly(4-styrenesulfonic acid) (SPS) (MW = 75K), sodium sulfate (Na_2SO_4), ammonium hydroxide (NH_4OH) (25%), hydrogen peroxide (H_2O_2) (30%), and sulfuric acid were purchased from Sigma Aldrich (St. Louis, MO). Hydrochloric acid (HCl) was purchased from VWR Scientific (Edison, NJ). Polyethyleneimine, branched (BPEI) (MW = 70K) was purchased from PolySciences, Inc. All chemicals were used as received. Gold-coated silicon wafers (AU.1000.SL1) comprising a 1000 Å layer of gold with a 50 Å titanium adhesion layer were purchased from Platypus Technologies (Madison, WI).

S1.2 Preparation of polymer solutions

PVPON and TA solutions were prepared at concentrations of 0.5 mg/mL with 10 mM phosphoric acid. The pH of each solution was adjusted down to 2.0 with HCl. BPEI solutions were prepared at a concentration of 0.5 mg/mL with 10 mM phosphate buffer at pH 7.5. PAH and SPS solutions were prepared at concentrations of 10 mM with respect to the repeat units with 0.5 M NaCl and were adjusted to pH 2.0. Rinse water contained 10 mM phosphoric acid and was adjusted to pH 2.0 with HCl. Deionized (DI) water (18.2 MΩ-cm, Milli-Q Ultrapure Water System, Millipore) was used to prepare all solutions.

S1.3 Assembly of films

The gold-coated silicon wafers (typically 1 cm x 3 cm) were first immersed in a solution of H_2O/H_2O_2(30%)/NH_4OH(25%) (5:1:1) solution at 75-80°C for 5 min (*Caution: cleaning solution is highly reactive and caustic*), rinsed thoroughly with DI water, and then dried under a stream of nitrogen. Next, each substrate was electrochemically cycled in 0.5 M H_2SO_4 (~20 mL) from 0.2 V to 1.6 V (vs. a saturated calomel electrode (SCE)) with a Pt wire counter electrode in a three-electrode cell. This cyclic voltammetry (CV) procedure was carried out at scan rate of 1 V/s for 100 cycles, sufficient to give a stable CV curve. This process activates the gold surface by forming and reducing a gold oxide layer on the surface. Next, the substrates were rinsed thoroughly with DI water and then immersed in a BPEI solution (0.5 mg/mL, 10 mM phosphate buffer, pH 7.5) overnight.

Subsequently, the substrates were rinsed with DI water and coated with $(PVPON/TA)_{20}$ films using a StratoSequence VI dip coater (nanoStrata, Inc.). This process included a 5 min immersion in the PVPON solution, followed by three 1 min rinse steps. Next, the substrate was immersed in the TA solution for 5 min, followed by three additional 1 min rinse steps. This cycle was repeated to construct films comprising the desired number of layers. After assembly, films were rinsed with DI water and dried under a stream of nitrogen.

S1.4 Film thickness and morphology measurements

Film thickness was measured with spectroscopic ellipsometry using a J.A. Woollam (Lincoln, NE) M-2000 instrument. Data were fit using J.A. Woollam WVASE32 software. Since the Au layer on the Au-coated Si substrates is optically thick, only a two-layer model was required to fit the data; specifically, one layer for the gold substrate and one layer for the overlying polymer film. The optical constants of the gold were obtained through a point-by-point fit for refractive index (n) and extinction coefficient (k). The transparent polymer film ($k = 0$) was modeled as a Cauchy layer (two-term only: $n(\lambda) = A_n + B_n/\lambda$) in which the fitted parameters were film thickness, A_n, and B_n over the wavelength range 300-1000 nm. For films that exhibited a microporous morphology with a cloudy appearance, ellipsometric fits were improved by including Urbach absorption as part of the Cauchy model using WVASE32 software. An incident angle of 70° was used for all measurements. Film thickness was also checked with a Veeco Dektak 150 Surface Profiler with a stylus tip radius of 2.5 μm and an applied stylus force of 2 mg.

Film surface morphology was investigated with atomic force microscopy (AFM) using a Dimension 3100 Scanning Probe Microscope (Veeco Instruments, Plainview, NY) in tapping mode. PointProbe Plus AFM probes (Nanosensors, Neuchatel, Switzerland) with a nominal tip radius of less than 7 nm were used. Images were flattened and the root-mean-squared (RMS) surface roughness (R_q) was determined using Veeco Nanoscope version 6.13R1 software.

S1.5 Electrochemical dissolution studies and pH control studies

Electrochemical experiments were carried out with a Princeton Applied Research EG&G 263A potentiostat/galvanostat in a three-electrode cell. The electrolyte was ~20 mL of 10 mM Na_2SO_4, the working electrode was a conducting Au-coated silicon substrate (10 x 30 x 0.5 mm) coated with the polymer thin film, the reference electrode was an SCE (sat. KCl), and the counter electrode was a Pt wire. Three different dissolved oxygen concentrations were investigated. Saturated O_2 levels (~40 ppm) were attained by bubbling pure O_2 through the electrolyte for 30 min, while ambient O_2 levels (~8 ppm) were attained by aerating the solution by shaking. Oxygen was eliminated from solutions (<1 ppm) by bubbling pure N_2 through the solution for 30 min. Linear scan voltammetry, carried out at a scan rate of 50 mV/s, was executed to assess the current response at different voltages and for different dissolved oxygen levels. Potentiostatic experiments were carried out to induce film dissolution; current flow was measured over time (chronoamperometry), integrated to charge versus time (chronocoulometry), and normalized by the film area. After each experiment, films were rinsed with DI water and dried under a stream of nitrogen.

As a control, the pH-triggered dissolution of the films was studied by raising the *bulk* pH of the solution. Solutions containing 10 mM Na_2SO_4 were adjusted to pH 9, 9.5, and 10.0 by addition of dilute NaOH. Utilizing the procedure previously reported by Erel-Unal and Sukhishvili,[1] films were immersed in the high pH solution and intermittently removed and dried with nitrogen gas for a thickness measurement using spectroscopic ellipsometry.

S1.6 Free-standing film release

First, a $(PVPON/TA)_{20}$ film was assembled as described above. Next, a $(PAH/SPS)_{80}$ film was assembled atop the $(PVPON/TA)_{20}$ film using 10 min dips in the PAH and SPS baths, each followed by three, 1 minute rinses. A razor blade was then used to scratch the edges of the substrate to ensure that the film did not wrap around to the backside (not Au-coated) of the substrate. Next, an electric potential of -1.0 V (vs. SCE) was applied to the substrate in a 10 mM Na_2SO_4 electrolyte (8 ppm O_2) for 2 min with no stirring, at which point the electrolyte was gently stirred with a magnetic stirrer to facilitate release of the free-standing film.

S2. Supplementary Results and Discussion

S2.1 Electrochemical response of a gold-coated silicon electrode

Linear scan voltammograms acquired at a scan rate of 50 mV/s in a three-electrode cell reveal the electrochemical behavior of the gold surface (Fig. S1). Fig. S1A shows a potential scan down to -1.5 V (vs. SCE). Decomposition of the solvent, that is, reduction of water, proceeds at voltages lower than -1.0 V as evidenced by the drastic increase in current. Fig. S1B shows the same data, but only in the oxygen reduction region down to -1.0 V to emphasize the impact of dissolved oxygen concentration on the current flow. The first wave in the voltage range of approximately 0 V to -0.50 V (with dependence on oxygen concentration) is attributed to reduction of oxygen to hydrogen peroxide (Equation 1 in the main text), while the wave at more negative voltages is attributed to the direct reduction of oxygen to water (Equation 2 in the main text). Therefore, the oxygen reduction potential region is roughly 0 V to -1.0 V. Clearly, in this region, the current flow is a function of both oxygen concentration and the applied voltage. Since current flow is directly proportional to the rate of oxygen reduction, and thus the rate of generation of hydroxide ions at the electrode surface, we anticipated and indeed found that the dissolution rate of hydrogen-bonded thin films can be tuned using these variables (Fig. 1 in the main text).

At higher (anodic) voltages (not shown), only capacitive behavior was observed, which is not expected to affect local pH. Starting at +1.3 V, hydrolysis of water occured, which lowers the pH at the interface between the electrode and the film.

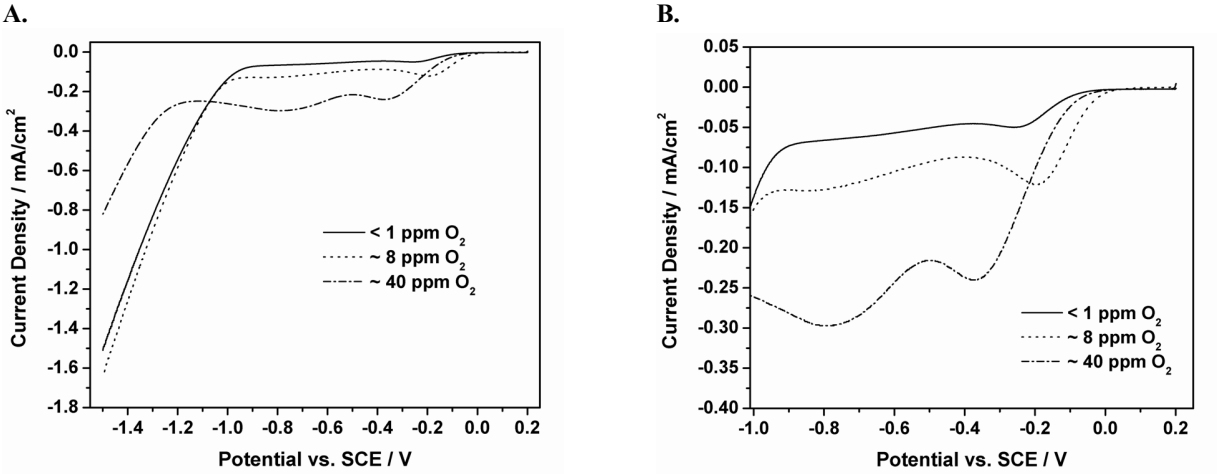

Fig. S1: Linear scan voltammograms (a) including the reduction of water (below -1 V) and (b) including only the oxygen reduction region (0 V to -1 V) of a gold-coated Si substrate at a scan rate of 50 mV/s in 10 mM Na_2SO_4 with different concentrations of dissolved oxygen.

S2.2 Spectroscopic ellipsometry measurements

Excellent fits were obtained to the experimental data using the Cauchy model as described above. Fig. S2A shows the experimental data and model fit for a $(PVPON/TA)_{20}$ film initially, before application of a voltage. Fig. S2B shows the same information for a film that has been electrochemically dissolved at -0.25 V for 7.5 min. The refractive index of each film at 633 nm is listed as an inset in each figure.

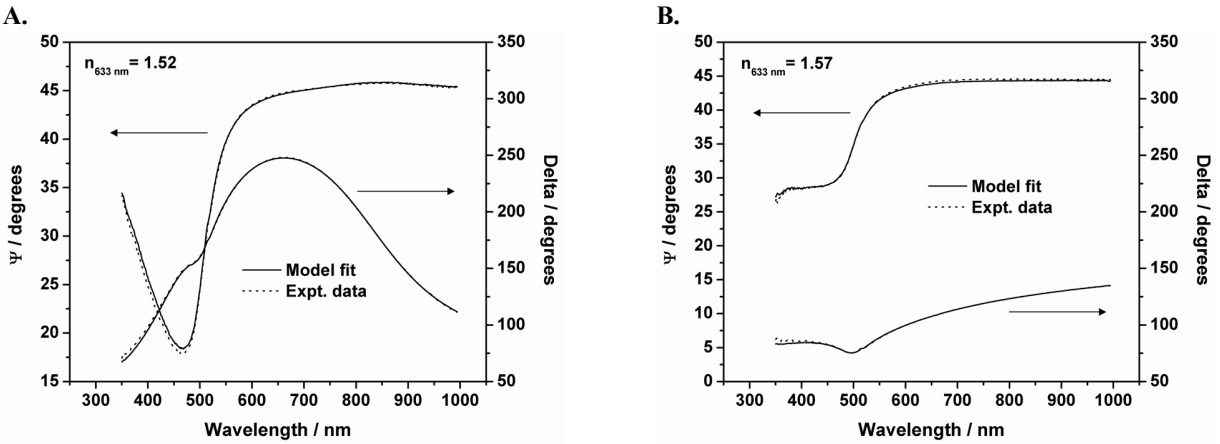

Fig. S2: Spectroscopic ellipsometry data and model fits for (a) a $(PVPON/TA)_{20}$ film initially (with thickness 149.2 ± 9.1 nm) and (b) the same film after application of -0.25 V (vs. SCE) for 7.5 min resulting in a thickness of 3.5 ± 0.2 nm.

S2.3 Chronocoulometry during film dissolution

The cumulative amount of charge injected into the submersed gold electrodes was measured over time during the application of different voltages (at 8 ppm O_2). The magnitude of the current at each time corresponds to the rate of the reaction occurring at the electrodes, while the total amount of charge injected up to a certain time is representative of the cumulative extent of reaction. Fig. S3 shows charge injected versus time for $(PVPON/TA)_{20}$ films subjected to voltages in the range -0.25 V to -1.5 V (vs. SCE). The time to 50% dissolution of the films (determined from linear interpolation between points in Fig. 1a of the main text) and the corresponding total charge injected at that time is listed in Table S1. Quantitative assessment of these results is complicated by the fact that oxygen reduction occurs through a complex reaction mechanism involving different pathways that are favored at different applied voltages and pH values.[2] At -0.50 V and -1.0 V, the total charge required to dissolve the film by 50% is very similar. At -0.25 V, significantly more charge is required to dissolve the film to the same extent, while at -1.5 V, reduction of water rapidly produces OH^- and significantly less charge is required to dissolve the film. Future modeling work will consider how the rate of OH^- generation and the influence of diffusion affect the time scale of local pH changes and the time scale for film dissolution.

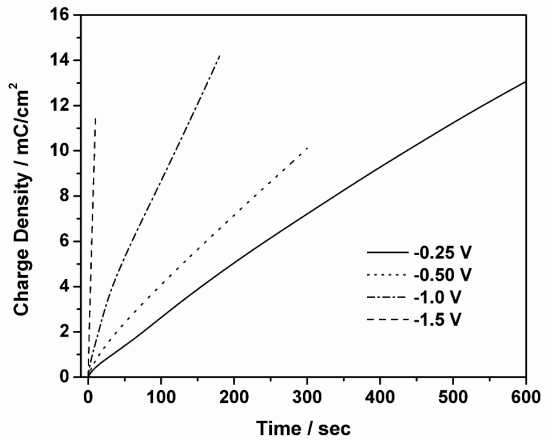

Fig. S3: Cumulative charge injected over time into gold electrodes coated with $(PVPON/TA)_{20}$ films at different applied voltages. The slope of each line corresponds to the current, that is, the rate of reaction (O_2 and/or H_2O reduction to OH^-).

Table S1: Comparison of the time to 50% dissolution and the total cumulative charge injected up to that time for $(PVPON/TA)_{20}$ films subjected to different voltages.

Potential (V)	Time to 50% Dissolution (sec)	Total Charge Required (mC/cm^2)
-0.25	351	8.28
-0.50	79.4	3.41
-1.0	23.7	3.08
-1.5	1.01	1.33

S2.4 Film surface morphology during dissolution

The surface morphology of the $(PVPON/TA)_{20}$ films was measured in the dry state for films as a function of time and applied potential. For reference, the AFM height images of the initial film and of bare gold are displayed in Fig. S4 and S5, respectively, at both height scales used in the subsequent figures. At applied potentials of -0.25 V and -0.50 V (with 8 ppm O_2) (Fig. S6) the film surface remains smooth (R_q < 4 nm) throughout the dissolution process. This observation is indicative of a top-down, or surface erosion mechanism.[3, 4] In contrast, at applied voltages of -1.0 V (with 8 ppm O_2) (Fig. S7) and -0.50 V (at 30 ppm O_2) (Fig. S8), the films develop a pitted morphology during the dissolution process. This observation is consistent with a bulk erosion mechanism, instead of a surface erosion mechanism.[3, 5] At more negative voltages, and at higher oxygen concentrations, the rate of oxygen reduction, and thus the rate of hydroxide ion generation is increased, as shown above. Therefore, it appears that a faster onset of increased local pH and/or possibly a higher local pH (subject of further study) results in both a more rapid decrease in film thickness and a rapid destabilization of the film structure.

The formation of pores indicates a thermodynamic instability, possibly a spinodal decomposition, as proposed by other authors for pH-induced porosity transitions in layer-by-layer films,[6] or a different "dewetting" mechanism involving the nucleation of holes in the film.[7, 8] In either case, when a locally high pH causes the deprotonation of the phenol groups in tannic acid, the cohesive hydrogen bonds in the film are broken. The polymer chains and tannic acid molecules are then free to explore the energy landscape and rearrange into a minimal energy conformation that results in the formation of pores. It appears that the pores grow with time and merge to form a "cellular" structure, as has been previously observed by Reiter for polystyrene films,[9] before the material dissolves into solution. The bumps or ridges observed around the edges of the pores have also been observed by others,[7, 8, 10] and are thought to comprise material formerly present in the interior of the pores. As an aside, the pores do reach the substrate. The average pore depth for a $(PVPON/TA)_{20}$ film subjected to -1.00 V for 20 sec was found to be 127 ± 18 nm (average from the measurement of 24 pores), determined via AFM. The thickness of the same film was measured to be 127 ± 10 nm with profilometry and 123 ± 14 nm with ellipsometry, identical to the pore depth.

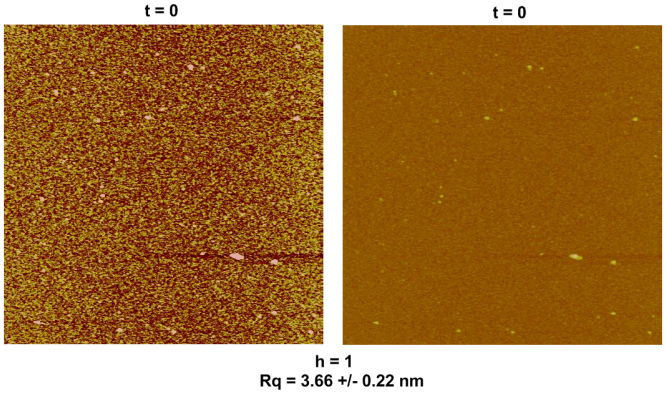

Fig. S4: AFM height images with scale 20 µm x 20 µm x 20 nm (left) and 20 µm x 20 µm x 200 nm (right) of initial $(PVPON/TA)_{20}$ films in the dry state. The normalized film thickness (h) and RMS roughness (Rq) are reported with ± one standard deviation from n = 5-7 measurements.

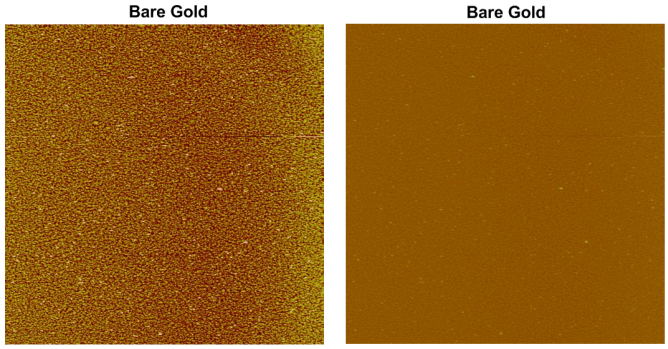

Fig. S5: AFM height images with scale 20 µm x 20 µm x 20 nm (left) and 20 µm x 20 µm x 200 nm (right) of bare, freshly cleaned gold-coated silicon slides in the dry state. The normalized film thickness (*h*) and RMS roughness (*Rq*) are reported with ± one standard deviation from n = 5-7 measurements.

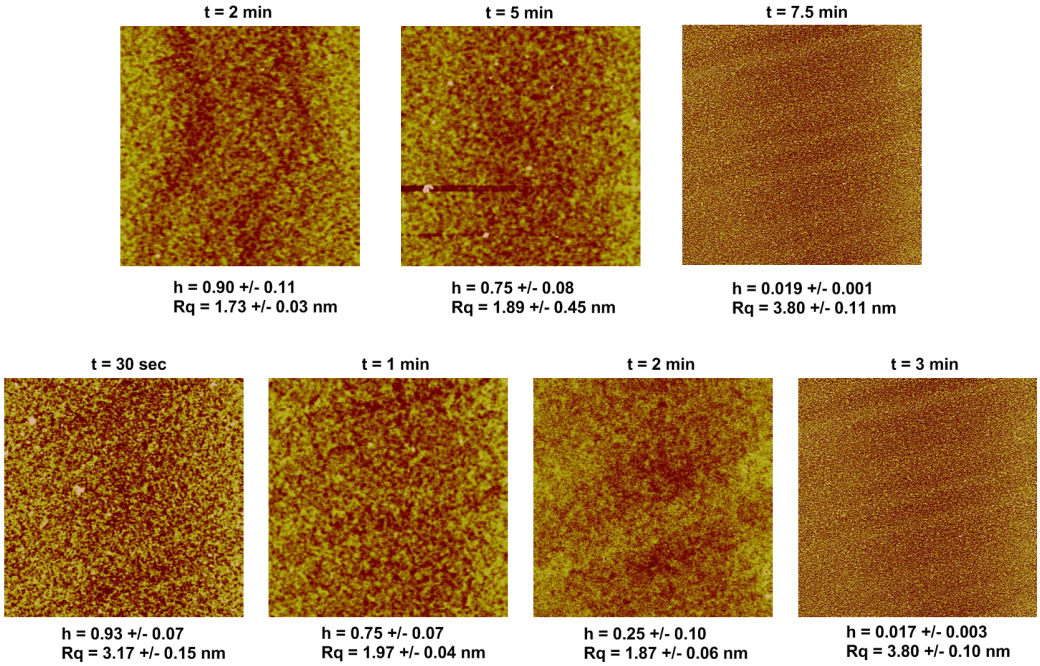

Fig. S6: AFM height images (scale 20 µm x 20 µm x 20 nm) of $(PVPON/TA)_{20}$ films in the dry state after application of -0.25 V (top row) and -0.50 V (bottom row) in a 10 mM Na_2SO_4 solution (8 ppm O_2) for the specified amounts of time. The normalized film thickness (*h*) and RMS roughness (*Rq*) are reported for each image. Values are reported with ± one standard deviation from n = 5-7 measurements. At these mild voltages, the films appear to degrade by a homogeneous, top-down surface erosion mechanism.

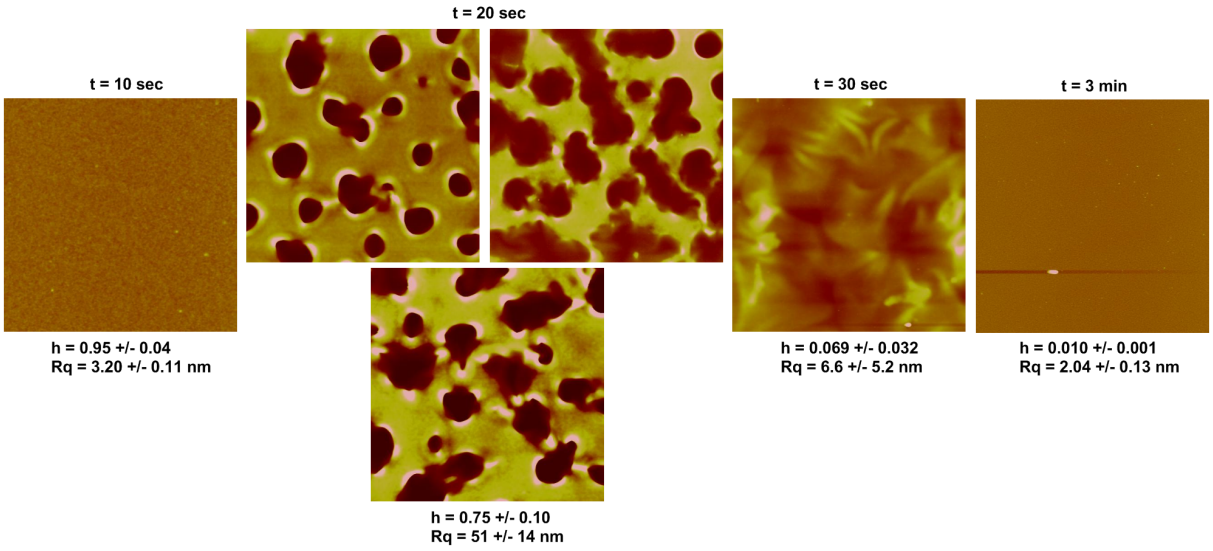

Fig. S7: AFM height images (scale 20 µm x 20 µm x 200 nm) of $(PVPON/TA)_{20}$ films in the dry state after application of -1.00 V in a 10 mM Na_2SO_4 solution (8 ppm O_2) for the specified amounts of time. The normalized film thickness (*h*) and RMS roughness (*Rq*) are reported for each image. Values are reported with ± one standard deviation from n = 5-7 measurements. At this more negative voltage, the films develop a porous morphology indicative of a phase separation and they appear to degrade by a heterogeneous bulk erosion mechanism. At t = 20 sec, the films were not spatially homogenous; thus, images from different locations on the film are provided.

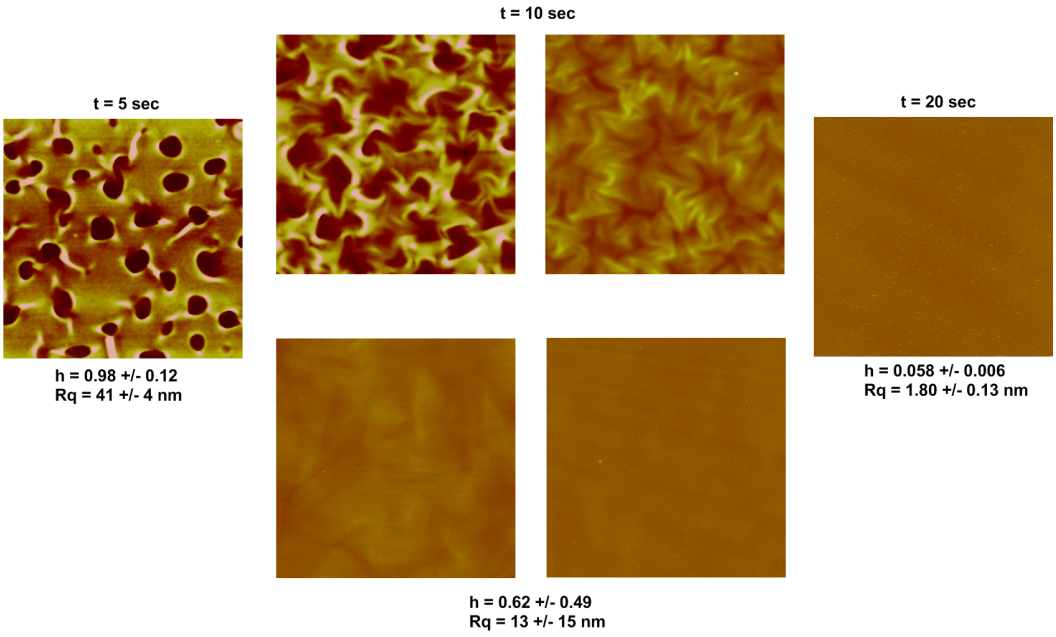

Fig. S8: AFM height images (scale 20 µm x 20 µm x 200 nm) of $(PVPON/TA)_{20}$ films in the dry state after application of -0.50 V in a 10 mM Na_2SO_4 solution (30 ppm O_2) for the specified amounts of time. The normalized film thickness (*h*) and RMS roughness (*Rq*) are reported for each image. Values are reported with ± one standard deviation from n = 5-7 measurements. At this elevated concentration of dissolved oxygen, a potential of -0.50 V more rapidly increases local pH and leads to a different film erosion mechanism. As at -1.00 V with 8 ppm O_2, the films develop a porous morphology indicative of a phase separation and they appear to degrade by a heterogeneous bulk erosion mechanism. At t = 10 sec, the films were not spatially homogenous; thus, images from different locations on the film are provided.

S2.5 Free-standing film characterization

The $(PVPON/TA)_{20}(PAH/SPS)_{80}$ composite film thickness was measured to be approximately 397 ± 11 nm with profilometry and 412 ± 13 nm with spectroscopic ellipsometry. After application of -1.0 V (vs. SCE) for 2 min, the film would not release from the substrate without mechanical agitation. Therefore, gentle magnetic stirring was initiated, which caused the film to peel off the substrate as a single sheet. While the film did have a tendency to fold upon itself, it was possible to capture the film on a microscope slide and to measure the thickness of a single film layer (and multiple layers) with profilometry (Fig. 3 in the main text). The thickness of the $(PAH/SPS)_{80}$ free-standing film was measured to be 238 ± 17 nm, while the thickness of the sacrificial $(PVPON/TA)_{20}$ layers before deposition of the overlying $(PAH/SPS)_{80}$ film was measured to be 149 ± 14 nm. Considering the thickness of the composite $(PVPON/TA)_{20}(PAH/SPS)_{80}$ film given above, the expected thickness for the free-standing film, assuming complete dissolution of the sacrificial layers would be 263 ± 20 nm. This value matches well with the actual measured thickness of the free-standing film, which implies complete or nearly complete dissolution of the sacrificial layers.

S2.6 Control: Bulk pH-triggered dissolution

Dissolution of the $(PVPON/TA)_{20}$ films induced by raising the *bulk* pH instead of the *local* pH confirmed that the film stability is indeed compromised by an increase in pH, as has been previously shown by Erel-Unal and Sukhishvili for $(PVPON/TA)_6$ films on silicon.[1] Figure S9 shows the normalized thickness of identical $(PVPON/TA)_{20}$ films on gold-coated silicon over time after submersion in 10 mM Na_2SO_4 solutions of pH 9, 9.5, and 10. While Erel-Unal and Sukhishvili found the critical disintegration pH (defined as the pH that causes ~50% of the film to dissolve after 20 min) to be 9.0, we observe a slightly higher critical dissolution pH between 9.0 and 9.5. It is possible that the difference in film thickness (~25 nm for 6 bilayer films and ~160 nm for 20 bilayer films), PVPON molecular weight (360K used by Erel-Unal compared to 1.3 million used by us), supporting electrolyte (phosphate buffer used Erel-Unal compared to sodium sulfate used by us), and/or substrate effects (silicon versus gold) may result in a slight shift in critical disintegration pH. Regardless, the electrochemical reduction of dissolved oxygen evidently raises the local pH above the critical disintegration pH for $(PVPON/TA)_{20}$ on gold, resulting in film dissolution. Deslouis et al. previously showed that reduction of dissolved oxygen on a gold mesh electrode in a 0.5 M K_2SO_4 solution resulted in an interfacial pH of 10.4-10.7,[11] well above the critical disintegration pH for the $(PVPON/TA)_n$ system.

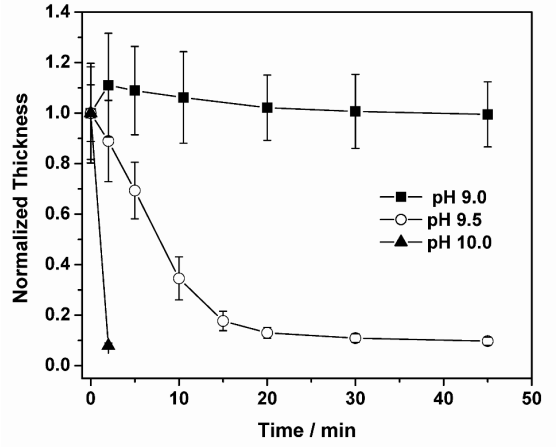

Fig. S9: Normalized thickness of three identical $(PVPON/TA)_{20}$ films exposed to different bulk pH conditions over time. Error bars represent ± one standard deviation from measurements taken at five different locations on each film.

References

1. I. Erel-Unal and S. A. Sukhishvili, *Macromolecules*, 2008, **41**, 3962-3970.
2. J. P. Hoare, *The Electrochemistry of Oxygen*, Interscience Publishers, New York, 1968.
3. N. J. Fredin, J. T. Zhang and D. M. Lynn, *Langmuir*, 2005, **21**, 5803-5811.
4. F. von Burkersroda, L. Schedl and A. Gopferich, *Biomaterials*, 2002, **23**, 4221-4231.
5. L. Lu, C. A. Garcia and A. G. Mikos, *J. Biomed. Mater. Res., Part A*, 1999, **46**, 236-244.
6. J. D. Mendelsohn, C. J. Barrett, V. V. Chan, A. J. Pal, A. M. Mayes and M. F. Rubner, *Langmuir*, 2000, **16**, 5017-5023.
7. R. Seemann, S. Herminghaus and K. Jacobs, *Phys. Rev. Lett.*, 2001, **86**, 5534-5537.
8. R. Xie, A. Karim, J. F. Douglas, C. C. Han and R. A. Weiss, *Phys. Rev. Lett.*, 1998, **81**, 1251-1254.
9. G. Reiter, *Phys. Rev. Lett.*, 1992, **68**, 75-78.
10. J. L. Lutkenhaus, K. McEnnis and P. T. Hammond, *Macromolecules*, 2008, **41**, 6047-6054.
11. C. Deslouis, I. Frateur, G. Maurin and B. Tribollet, *J. Appl. Electrochem.*, 1997, **27**, 482-492.